Probing new physics in $\Lambda_b \to \Lambda_c(\to \Lambda\pi)\tau\bar{\nu}$ decay *

Ria Sain[1,**]

[1]Indian Institute of Technology, North Guwahati, Guwahati 781039, Assam, India

Abstract. We study the 4-body angular distribution for $\Lambda_b \to \Lambda_c^+(\to \Lambda\pi^+)\ell^-\bar{\nu}$ decays and discuss various asymmetric and angular observables in the Standard Model and the new physics scenarios . Considering the new physics effects in $b \to c\tau^-\bar{\nu}_\tau$ transitions, we have constrained the new Wilson coefficients of the one operator and two operator scenarios from the available data on these decays. The two-operator scenario with scalar-pseudoscalar and tensor quark current provides the most plausible solution to the current data. Also, we have tested the new physics sensitivities (one or two-operator scenarios) of the different angular observables in $\Lambda_b \to \Lambda_c(\to \Lambda\pi^+)\tau^-\bar{\nu}_\tau$ decays and found correlations among them.

1 Introduction

Over the past few years, the flavour changing charged current (FCCC) decay $b \to c\ell^-\bar{\nu}$ has been extensively studied in both experimental and theory fronts. The baryonic decay $\Lambda_b \to \Lambda_c\ell^-\bar{\nu}$ could provide complementary information. We can extract $|V_{cb}|$ from the measurements of the rates in $\Lambda_b \to \Lambda_c\ell^-\bar{\nu}$ decays; at the same time, we can extract and test the NP sensitivity of the LFU ratio defined in these modes [2–14]. The Large Hadron collider has produced copious amounts of Λ_b, which provides us with a lot of information on its semileptonic decay. For instance, it has provided the first-ever branching fraction as [15]

$$\mathcal{B}(\Lambda_b \to \Lambda_c\tau^-\nu_\tau) = (1.50 \pm 0.16 \pm 0.25 \pm 0.23)\%. \tag{1}$$

In this article, we have done the angular analysis for $\Lambda_b^0 \to \Lambda_c^+(\to \Lambda\pi)\ell^-\bar{\nu}_\ell$ decay and made prediction for SM. Using the measurements on $R(D^{(*)})$, $R(\Lambda_c)$ along with $F_L^{D^*}$ we have done a frequentist analysis with one operator scenario, that can explain the current data simultaneously. We find that it is hard to explain all the data simultaneously if we take the predictions in the NP scenarios at their 1σ uncertainties. And if one tries with two operators at a time the situation improves and specific scenarios can explain all the data simultaneously within 1σ. And if correlation plots between the observables are studied then they will help us to predict the pattern of the measurements and how they can behave for updated measurements.

2 Formalism

2.1 Effective Hamiltonian

In the effective theory framework, the effective Hamiltonian is written in terms of the operators and the corresponding Wilson Coefficients (WC) for the semileptonic flavour changing

*Based on the paper [1] with Soumitra Nandi and Shantanu Sahoo

**e-mail: ria.sain.2013@gmail.com

charged current transition $b \to c\tau^-\bar{\nu}_\tau$ as

$$\mathcal{H}_{eff} = \frac{G_F V_{cb}}{\sqrt{2}}\Big\{\Big[(1+C_{V_1})\bar{c}\gamma_\mu(1-\gamma_5)b + C_{V_2}\bar{c}\gamma_\mu(1+\gamma_5)b\Big]\bar{\tau}\gamma^\mu(1-\gamma_5)\nu_\tau + \Big[C_{S_1}\bar{c}(1+\gamma_5)b + C_{S_2}\bar{c}(1-\gamma_5)b\Big]\bar{\tau}(1-\gamma_5)\nu_\tau + \Big[C_T\bar{c}\sigma^{\mu\nu}(1-\gamma_5)b\Big]\bar{\tau}\sigma_{\mu\nu}(1-\gamma_5)\nu_\tau\Big\}, \tag{2}$$

where G_F is the Fermi constant, V_{cb} is the Cabibbo-Kobayashi-Maskawa (CKM) matrix element, and we use $\sigma_{\mu\nu} = i[\gamma_\mu, \gamma_\nu]/2$. All the information about short-distance physics and possible new physics effects are contained in the Wilson coefficients . As standard literature in the absence of New Physics, the C_i's are zero.

2.2 Angular distribution and Observables

The four-fold differential decay rate of $\Lambda_b \to \Lambda_c^+(\to \Lambda\pi^+)\ell\,\bar{\nu}_\ell$ decay, with a unpolarized Λ_b baryon, is fully parameterized in terms of q^2 and the three angles. The angle θ_ℓ is defined between the leptons and the direction to the Λ_c baryon in the virtual W-boson rest frame and the angle θ_Λ is between the Λ baryon and direction of the Λ_c baryon in the rest frame of Λ_c. The azimuthal angle ϕ is defined as an angle between the two decay planes spanned by W^*-ℓ and Λ_c-Λ_b system in the Λ_b rest frame. The measurable 4-fold angular decay distribution can then be written as

$$\frac{d^4\Gamma}{dq^2 d\cos\theta_\ell d\cos\theta_\Lambda d\phi} = \frac{3}{8\pi}K(q^2, \cos\theta_\ell, \cos\theta_\Lambda, \phi) \tag{3}$$

where the angular distribution $K(q^2, \cos\theta_\ell, \cos\theta_\Lambda, \phi)$ depends only on the di-lepton invariant mass square, q^2, and contains the hadronic information which in turn is expressed in terms of the hadronic helicity amplitude, parametrized by WC's and baryonic form factors, and can be expressed as follows:

$$\begin{aligned} K(q^2, \cos\theta_\ell, \cos\theta_\Lambda, \phi) = {} & (K_{1ss}\sin^2\theta_\ell + K_{1cc}\cos^2\theta_\ell + K_{1c}\cos\theta_\ell) \\ & + (K_{2ss}\sin^2\theta_\ell + K_{2cc}\cos^2\theta_\ell + K_{2c}\cos\theta_\ell)\cos\theta_\Lambda \\ & + (K_{3sc}\sin\theta_\ell\cos\theta_\ell + K_{3s}\sin\theta_\ell)\sin\theta_\Lambda\cos\phi \\ & + (K_{4sc}\sin\theta_\ell\cos\theta_\ell + K_{4s}\sin\theta_\ell)\sin\theta_\Lambda\sin\phi\,. \end{aligned} \tag{4}$$

The expressions for the K_i's are written in terms of helicity amplitudes which are expressed in terms of Wilson coefficients, form factors and constants [1]. By integrating over the lepton-side angle θ_ℓ and the azimuthal angle ϕ we can obtain the two-fold differential decay rate as follows-

$$\frac{\mathrm{d}^2\Gamma}{\mathrm{d}q^2\mathrm{d}\cos\theta_\Lambda} = \frac{1}{2}\frac{\mathrm{d}\Gamma}{\mathrm{d}q^2}(1 + \alpha_\Lambda\, P_{\Lambda_c}\cos\theta_\Lambda) \tag{5}$$

where, P_{Λ_c} represents the Λ_c spin polarization, which defined as

$$P_{\Lambda_c} = \frac{\mathrm{d}\Gamma^{\lambda_{\Lambda_c}=1/2}/\mathrm{d}q^2 - \mathrm{d}\Gamma^{\lambda_{\Lambda_c}=-1/2}/\mathrm{d}q^2}{\mathrm{d}\Gamma/\mathrm{d}q^2}. \tag{6}$$

Here, $\frac{\mathrm{d}\Gamma}{\mathrm{d}q^2}^{\lambda_{\Lambda_c}=\pm1/2}$ are the differential decay rates for the polarized intermediate state Λ_c baryon Further integrating over the hadronic angle θ_Λ, we can obtain the following differential decay

rate depending only on q^2.

$$\frac{d\Gamma}{dq^2} = 2K_{1ss} + K_{1cc} \tag{7}$$

In experiments all the angular asymmetries are measured as normalised by the decay rate, which we define

$$\hat{K}_i = \frac{K_i}{2K_{1ss} + K_{1cc}} \tag{8}$$

Also, we have constructed another asymmetric observable associated with the lepton polarization λ_ℓ, in particular, the lepton-polarization asymmetry:

$$P_\ell^{(\Lambda_c)} = \frac{\mathrm{d}\Gamma^{\lambda_\ell=1/2}/\mathrm{d}q^2 - \mathrm{d}\Gamma^{\lambda_\ell=-1/2}/\mathrm{d}q^2}{\mathrm{d}\Gamma/\mathrm{d}q^2}\,. \tag{9}$$

For explicit expression of $\frac{\mathrm{d}\Gamma}{\mathrm{d}q^2}^{\lambda_\ell=\pm1/2}$, Also, we have obtained the convexity parameter C_F^ℓ defined by

$$C_F^\ell = \frac{1}{d\Gamma/dq^2}\left(\frac{d}{d(\cos\theta_l)}\right)^2\left(\frac{d^2\Gamma}{dq^2 d\cos\theta_l}\right). \tag{10}$$

3 Test of New Physics with existing observations

A few other lepton flavor violating ratios, like $R(D^{(*)}) = \Gamma(B \to D^{(*)}\tau^-\bar{\nu})/\Gamma(B \to D^{(*)}\ell^-\bar{\nu})$ and $R(J/\psi) = \Gamma(B_c \to J/\psi\tau^-\bar{\nu})/\Gamma(B_c \to J/\psi\ell^-\bar{\nu})$ are measured by the experimental collaborations BaBar, Belle, and LHCb, respectively [16–26]. A global average of these quantities is available HFLAV [27], $R(D) = 0.357 \pm 0.029$ and $R(D^*) = 0.284 \pm 0.012$. Based on the most recent lattice inputs, the corresponding SM predictions are given by $R(D)_{SM} = 0.304 \pm 0.003$ and $R(D^*)_{SM} = 0.258 \pm 0.012$.[28]

At the moment, the measurements have relatively large errors, and the SM prediction of $R(D^*)$ has a relatively large error as compared to $R(D)$. In the present scenario, the data deviates from the respective SM predictions at $\approx 2\sigma$. Note that, the measurements on $R(D)$ and $R(D^*)$ also have some correlation due to which there will be little more discrepancies than 2σ [27].

Recently, LHCb has measured $\mathcal{B}(\Lambda_b \to \Lambda_c\tau\bar{\nu})$ and finds [15],

$$R(\Lambda_c) = 0.242 \pm 0.026 \pm 0.040 \pm 0.059 \tag{11}$$

where the first uncertainty is statistical, the second is systematic and the third is due to external branching fraction measurements. In comparison to our SM prediction,

$$R(\Lambda_c)_{SM} = 0.330 \pm 0.010, \tag{12}$$

it points towards a downward shift. The data is consistent with the SM prediction within 1.15-σ uncertainties.

Note that in the measurement for $R(\Lambda_c)$, to normalize $\Lambda_b \to \Lambda_c\tau\nu$ decay rate, LHCb have used $\mathcal{B}(\Lambda_b \to \Lambda_c\mu\nu)_{\mathrm{DELPHI}}$= 6.2(1.4)% which is measured by DELPHI collaboration [29]. Using this data we have obtained an estimate for $|V_{cb}|$ which is as given below

$$|V_{cb}| = (37.9 \pm 4.5) \times 10^{-3}. \tag{13}$$

This estimate has large error but consistent with those obtained from $B \to D^{(*)}(\mu, e)\nu$ modes [28]. At the same time we have utilised the measured value $\mathcal{B}(\Lambda_b \to \Lambda_c \tau\nu) = (1.5 \pm 0.16 \pm 0.25 \pm 0.23)\%$ [15] and have obtained

$$|V_{cb}| = (44.0 \pm 5.0) \times 10^{-3}. \tag{14}$$

Both of these estimates are consistent within their 0.91σ uncertainties, though they have large errors and there is a gap of about 16% between the two best fit values. In the context of NP effects in these modes, it is important to note that $\Lambda_b \to \Lambda_c \tau\nu$ could be potentially sensitive to contributions beyond the SM.

In the following subsections, we will discuss the results of the analyses of the extractions of new physics from different fits to the available data.

3.1 New Physics analysis: One operator scenario

The new physics effective operators relevant to $b \to c\tau^-\bar{\nu}$ transitions are defined in eqn.2. The relevant data on $B \to D^{(*)}\mu^-\bar{\nu}$ decays suggest that the allowed new physics contributions in $b \to c\mu^-\bar{\nu}$ transitions are negligibly small [28], which is as per the expectations. To constrain the new WCs, we first do the fit to the available data considering the contributions from one operator at a time. We perform a combine analysis of $R(D)$, $R(D^*)$, $R(\Lambda_c)$, $F_L^{D^*}$ and $\mathcal{B}(\Lambda_b \to \Lambda_c \tau\nu)$ observables. We have used global average data (central value and uncertainty) for $R(D)$ and $R(D^*)$ observables along with their correlation, which were computed by the Heavy Flavor Averaging Group (HFLAV) [27], as input in our analysis. Furthermore, we included the latest LHCb measurement, which is the only single measurement, for the data on $\mathcal{B}(\Lambda_b \to \Lambda_c \tau\nu)$ and $R(\Lambda_c)$ [15]. In addition, we have incorporated the recent measurement on $F_L^{D^*}$ by LHCb [30]. In table 1, we have presented the data used in the fit along with the corresponding references.

$R(D)$ [27]	$R(D^*)$ [27]	correlation [27]	$R(\Lambda_c)$ [15]	$\mathcal{B}(\Lambda_b \to \Lambda_c \tau\bar{\nu}_\tau)$ [15]	$F_L^{D^*}$ [30]
0.357(29)	0.284(12)	−0.37	0.242(76)	0.015(4)	0.43(7)

Table 1: Experimental data used in the χ^2 analysis.

We closely follow the treatment in ref [28] for the observables $R(D)$, $R(D^*)$ and $F_L^{D^*}$. For our purposes, we have taken the analytic expressions for the observables $R(D)$ and $R(D^*)$ as well as $F_L^{D^*}$ from that reference. The new WCs are the only free parameters in these expressions. We also quote the error in SM predictions, which are shown as the overall normalization in the respective expressions. In the analysis in [28], the shape of the form factors is obtained using only the lattice inputs, and the estimated errors in SM are solely due to the form factors. In the NP scenarios, the additional error will come from the uncertainties in the fitted values of the new WCs. The shape of the $B \to D$ transition form factors are obtained using the lattice inputs from Fermilab-MILC collaboration [31] and the HPQCD collaboration [32]. For the $B \to D^*$ decay, the inputs on the form factors are taken from the Fermilab-MILC and JLQCD collaboration [33, 34]. For $\Lambda_b \to \Lambda_c \tau^-\bar{\nu}$ decay we have obtained the shape of all the form factors relevant in NP scenarios from lattice [2, 5]. In addition to $R(D)$, $R(D^*)$, $R(\Lambda_c)$ and longitudinal polarization $F_L^{D^*}$, we have used the total branching fraction $\mathcal{B}(\Lambda_b \to \Lambda_c \tau\bar{\nu}_\tau)$ as input in our analysis.

To perform a model-independent analysis, we did the χ^2-fit to the data given in table 1 with different NP hypothesis. The χ^2 function is defined as

$$\chi^2(C_k) = \sum_{i,j} [O_i^{th}(C_k) - O_i^{exp}](V^{exp} + V^{th})^{-1}_{i,j}[O_i^{th}(C_k) - O_i^{exp}]. \tag{15}$$

We have minimized this χ^2 function. Here, O_i^{exp} and O_i^{th} are the respective measured values and the theoretical expressions of the observables, and C_k's are the Wilson coefficients of the effective Hamiltonian in eqn. 2. $V_{i,j}^{exp(th)}$ is the corresponding measured (theoretical) covariance matrix. Therefore, observable uncertainties and their correlation can be taken care of through the covariance matrix. Here, the theory correlations will be between $R(D^*)$ and $F_L^{D^*}$, and between $R(\Lambda_c)$ and $\mathcal{B}(\Lambda_b \to \Lambda_c \tau\nu)$.

Parameter	One Parameter fit scenario			σ_{dev} (in σ)		
	Fit values	$\chi^2_{min.}$/DOF	P-Value	$R(D)$	$R(D^*)$	$R(\Lambda_c)$
$Re[C_{S_1}]$	0.104(45)	4.463/4	0.215	0.151	1.355	1.372
$Re[C_{S_2}]$	0.101(47)	5.187/4	0.159	0.098	1.709	1.297
$Re[C_{V_1}]$	0.050(22)	4.001/4	0.261	0.683	0.048	1.524
$Re[C_{V_2}]$	-0.0045(339)	9.176/4	0.027	1.564	1.029	1.128
$Re[C_T]$	-0.022(18)	7.903/4	0.048	1.971	0.343	1.385

Table 2: The simultaneous fit of the new physics WCs (one operator scenario) and the form factor. The inputs are $R(D)$, $R(D^*)$, $R(\Lambda_c)$, $F_L^{D^*}$, $\mathcal{B}(\Lambda_b \to \Lambda_c \tau\nu)$. These fit consider NP only in τ lepton final state. Also, we quantify the tension between observable and corresponding observational data for each scenario and present it in the unit of σ in the last three columns.

Observables	Observables Prediction (One operator scenario)					Expt. Measurement
	$Re[C_{S_1}]$	$Re[C_{S_2}]$	$Re[C_{V_1}]$	$Re[C_{V_2}]$	$Re[C_T]$	
$R(D)$	0.363(27)	0.361(29)	0.335(14)	0.301(21)	0.299(5)	0.357(29) [27]
$R(D^*)$	0.261(12)	0.255(12)	0.285(17)	0.260(20)	0.276(20)	0.284(12) [27]
$R(\Lambda_c)$	0.348(14)	0.342(13)	0.361(18)	0.329(13)	0.352(23)	0.242(76)[15]
$F_L^{D^*}$	0.433(3)	0.421(3)	0.427(9)	0.427(3)	0.421(6)	0.430(70) [30]
$P^\tau(D^*)$	-0.502(10)	-0.535(9)	-0.519(7)	-0.519(7)	-0.505(14)	-0.38(54) [21]
$P^\tau(D)$	0.433(42)	0.431(45)	0.324(3)	0.324(3)	0.336(10)	N.A.

Table 3: Predictions of $R(D)$, $R(D^*)$, $R(\Lambda_c)$ and $F_L^{D^*}$ using the corresponding fit results from table 2 while considering new physics only in τ channel.

3.2 New physics analysis: Two operators scenario

Following the discussion in the last subsection, we have separately studied the impact of the two-operator scenarios. Also, while analysing the contributions to the decay rate due to scalar, pseudoscalar, and tensor type operators, we have noticed terms which are due to the interference between different operators (like $C_i C_j$), and those terms are dependent on m_ℓ. So for $m_\ell = m_\mu$ these terms will be small can be ignored, but for $m_\ell = m_\tau$, while considering the NP present one at a time to our theory, these massive contributions remain left out. Hence, the study of the two operator scenarios will be important to incorporate and understand the impact of these mass-dependent interference terms, which will be otherwise missing in the one operator scenarios. Also, for simplicity we have considered only the real WCs.

We provide a detailed discussion for each of the angular distributions in the presence of one and two NP operators along with SM. In our analysis, we normalize each observable with the decay rate, which is $2K_{1ss} + K_{1cc}$. This makes the observables independent of $|V_{cb}|$. The

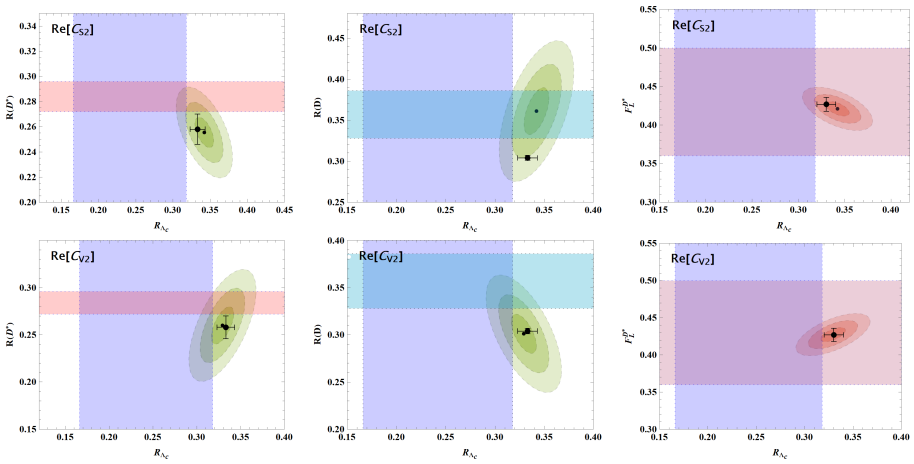

Figure 1: The correlation of $R(D)$, $R(D^*)$, $F_L^{D^*}$ with $R(\Lambda_c)$ in different one-parameter scenarios. The horizontal and vertical color bands represent the respective experimental results at their 1σ CI. The correlations between the observables are represented by ellipses. We have shown the 1σ, 2σ, and 3σ contour error bands around the best estimate point (black) using the best-fit point (given in table 2). The SM estimation has also been shown using a black point with vertical and horizontal 1σ error bars for the respective observables.

observables are then dependent only on the hadronic helicity amplitude, which is parameterized by form factors. In the subsequent section, we use the BCL parameterization for form factor shape. To check the NP sensitivities of these observables, using the form factors as an external input, we obtain the q^2 shapes of the observables under consideration. The table 4 presents our fit results for each two-parameter scenario. Among these we compare the predictions of $R(D)$, $R(D^*)$, $F_L^{D^*}$ and $R(\Lambda_c)$ with the respective measured values and estimated the deviations (σ_{dev}) using the formula given in [1]. Note that if we consider the 1σ error in the respective predictions, in all the two operator scenarios we can explain the measured observables in $B \to D^{(*)}\tau^-\bar{\nu}$ decays. However, the scenario with $[O_{S_2}, O_T]$ is the only two-operator scenario which could accommodate the data on $R(\Lambda_c)$ alongside $R(D)$, $R(D^*)$, $F_L^{D^*}$ within their 1σ uncertainties. This is also the best-fit scenario which has the largest p-value i.e., 67% among all others. The correlations between the observables in the scenario $[O_{S_2}, O_T]$ are shown in fig. 2 which indicates that we can comfortably explain all the four data mentioned above along with $P^\tau(D^*)$, which has a relatively large error. We have also analysed the correlation between these observables in all the other two operator scenarios and noted that it is possible to simultaneously explain the data on $R(\Lambda_c)$ with $R(D)$, $F_L^{D^*}$ and $P^\tau(D^*)$, respectively if we take the 3σ contours of our predictions. However, while it is coming to a simultaneous explanation of $R(\Lambda_c)$ and $R(D^*)$, most of the scenarios fail to do so even if we consider the 3σ contours. There are too many such plots, and we have not shown them here separately. We have estimated the σ level discrepancies between the prediction in the NP scenarios and the SM. We present the corresponding results in table 5, and the scenarios showing discrepancies of more than 2σ level are pointed in bold font. Note that in the two operator scenarios, we observe discrepancies in a couple of observable which we don't see in one operator scenarios. This is due to interference terms of the two new WCs proportional to the mass of the τ-lepton which are absent in the one operator scenarios.

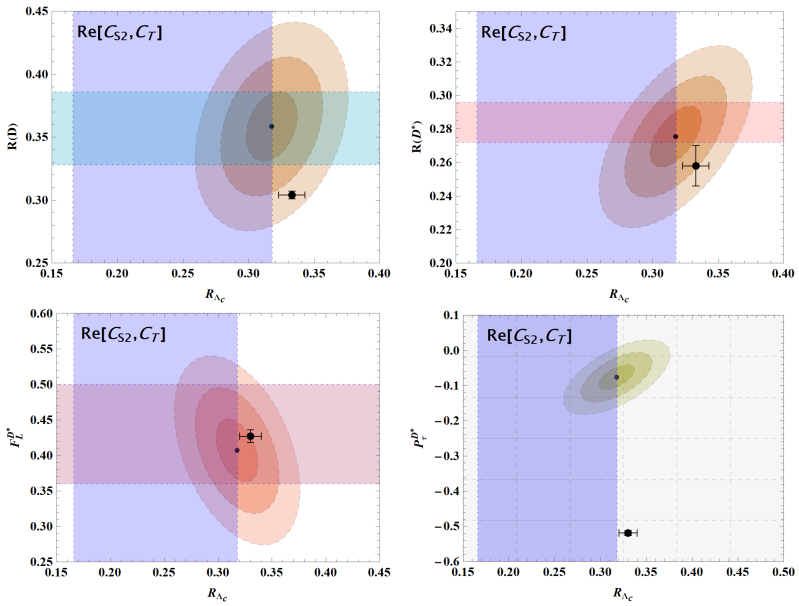

Figure 2: The plot shows the correlation between $R(D)$ and $R(\Lambda_c)$ in different NP two-parameter scenarios. The horizontal and vertical color bands represent the experimental constraints of $R(D)$ and $R(\Lambda_c)$, respectively, at a 1σ confidence level. The correlations between the observables are represented by an ellipse. We have also shown 1σ, 2σ, and 3σ contour error bands around the best estimate point (black) using the best-fit point (given in Table 4). The SM estimation has also been shown using a black point with vertical and horizontal 1σ error bars for the respective observables.

Note that apart from $[O_{S_1}, O_{S_2}]$, $[O_{S_2}, O_T]$ and $[O_{V_1}, O_{V_2}]$ in the rest of the two operator scenarios we do not observe any significant deviations in these observables with respect to the SM. Note that in the scenario $[O_{S_2}, O_T]$, apart from $A_{FB}^{\Lambda_c\tau}$ almost all the other observables will show discrepancies for the corresponding SM predictions. In the scenario $[O_{S_1}, O_{S_2}]$ we will observe deviations only in $\hat{K}_{3s}$, A_{FB}^{τ} and $A_{FB}^{\Lambda_c\tau}$ which is significant in A_{FB}^{τ}. The predictions of A_{FB}^{τ} and $A_{FB}^{\Lambda_c\tau}$ are lower than the SM and have opposite signs, while the prediction of $\hat{K}_{3s}$ is larger than the SM. In the scenario $[O_{V_1}, O_{V_2}]$, apart from $\hat{K}_{1cc}$, $\hat{K}_{1ss}$ and $P_\tau^{(\Lambda_c)}$ in the predictions of the rest of the observables we have noticed discrepancies. Also, here in a couple of observables, we see the predicted values are lower than and have opposite signs, and the rest are higher than SM. Therefore, once we have precise measurements of all these observables, a comparative study will be helpful to distinguish these three types of scenarios.

In addition, we have studied the q^2 distributions of all the asymmetric and angular observables in the two operator scenarios and presented them in fig. 3. These distributions will be helpful to test the NP sensitivities specific to the q^2 regions, which are otherwise missing in the q^2 integrated observables and can be compared with the measurements in small bins in the near future. We have taken the numerical values of the WCs from our fit results of two operator scenarios given in table 4. As obtained in table 5, we note sizeable NP effects in the

2 Operator	Two operator scenarios fit results				σ_{dev} (in σ)			
Scenario	WC fit results		χ^2_{min}/DOF	P-Value	$R(D)$	$R(D^*)$	$R(\Lambda_c)$	$F_L^{D^*}$
C_{S_1}, C_{S_2}	$Re[C_{S_1}]$	-2.268(207)	3.432/3	0.330	0.067	0.409	1.437	0.237
	$Re[C_{S_2}]$	0.904(220)						
C_{S_1}, C_T	$Re[C_{S_1}]$	0.098(46)	3.978/3	0.264	0.038	0.526	1.494	0.010
	$Re[C_T]$	-0.014(19)						
C_{S_2}, C_T	$Re[C_{S_2}]$	**-1.255(64)**	**1.553/3**	**0.670**	**0.039**	**0.391**	**0.963**	**0.278**
	$Re[C_T]$	**0.226(32)**						
C_{V_1}, C_{V_2}	$Re[C_{V_1}]$	-0.978(32)	3.557/3	0.313	0.113	0.303	1.503	0.013
	$Re[C_{V_2}]$	1.055(23)						
C_{V_1}, C_T	$Re[C_{V_1}]$	0.077(31)	2.827/3	0.419	0.148	0.466	1.296	0.006
	$Re[C_T]$	0.037(37)						
C_{V_2}, C_T	$Re[C_{V_2}]$	0.080(53)	5.829/3	0.120	0.435	0.560	1.634	0.389
	$Re[C_T]$	-0.059(28)						
C_{S_1}, C_{V_1}	$Re[C_{S_1}]$	0.051(73)	3.534/3	0.316	0.102	0.311	1.498	0.0004
	$Re[C_{V_1}]$	0.033(34)						
C_{S_1}, C_{V_2}	$Re[C_{S_1}]$	0.123(48)	3.511/3	0.319	0.106	0.301	1.494	0.098
	$Re[C_{V_2}]$	-0.033(33)						
C_{S_2}, C_{V_1}	$Re[C_{S_2}]$	0.045(65)	3.533/3	0.316	0.101	0.311	1.496	0.079
	$Re[C_{V_1}]$	0.038(29)						
C_{S_2}, C_{V_2}	$Re[C_{S_2}]$	0.139(54)	3.474/3	0.324	0.104	0.292	1.489	0.098
	$Re[C_{V_2}]$	-0.048(36)						

Table 4: Fit results for the simultaneous fit of the NP Wilson coefficients (in the two-operator scenario) and form-factor parameters. The inputs used in the fit are $R(D)$, $R(D^*)$, $R(\Lambda_c)$, $F_L^{D^*}$ and $\mathcal{B}(\Lambda_b \to \Lambda_c \tau \bar{\nu}_\tau)$, where we only consider new physics in the τ final state. In addition, we quantify the influence of LFUV data on the corresponding fit and present the results in the last three columns.

	Deviations w.r.t. SM predictions (in σ level)											
Scenario	$\hat{K}_{1cc}$	$\hat{K}_{1ss}$	$\hat{K}_{2cc}$	$\hat{K}_{2ss}$	$\hat{K}_{3sc}$	$\hat{K}_{3s}$	A_{FB}^{τ}	$A_{FB}^{\Lambda_c \tau}$	$A_{FB}^{\Lambda_c}$	P_{Λ_c}	$P_\tau^{(\Lambda_c)}$	C_F^τ
$[C_{S_1}, C_{S_2}]$	0.354	0.819	0.193	0.082	0.277	**4.22**	**20.051**	**9.856**	0.161	0.16	0.806	0.60
$[C_{S_1}, C_T]$	0.894	0.819	0.24	0.288	0.354	0.664	0.983	0.647	0.364	0.714	1.574	0.868
$[C_{S_2}, C_T]$	**3.328**	**4.915**	**6.209**	**5.794**	**2.683**	**2.507**	**6.116**	0.2	**7.343**	**7.532**	**8.831**	**4.389**
$[C_{V_1}, C_{V_2}]$	0.	0.	**13.133**	**13.136**	**12.021**	**4.468**	**19.279**	**9.753**	**18.11**	**70.863**	0.472	0.236
$[C_{V_1}, C_T]$	0.555	0.819	0.44	0.453	0.277	0.547	0.123	0.651	0.602	1.317	0.451	0.745
$[C_{V_2}, C_T]$	0.447	0.819	0.901	0.899	0.832	0.868	1.057	0.108	1.185	1.805	1.143	0.589
$[C_{S_1}, C_{V_1}]$	0.354	0.	0.	0.	0.	0.39	0.43	0.462	0.	0.	0.636	0.217
$[C_{S_1}, C_{V_2}]$	0.894	0.819	0.096	0.136	0.354	0.208	0.921	0.7	0.188	0.786	1.611	0.868
$[C_{S_2}, C_{V_1}]$	0.	0.	0.064	0.054	0.	0.469	0.193	0.325	0.081	0.324	0.572	0.118
$[C_{S_2}, C_{V_2}]$	0.894	0.819	0.354	0.36	0.354	0.139	0.064	0.217	0.497	1.658	1.089	0.759

Table 5: The discrepancies/agreement between the predictions in the two-operator scenarios and in the SM.

observables only for the scenarios $[O_{S_1}, O_{S_2}]$, $[O_{S_2}, O_T]$ and $[O_{V_1}, O_{V_2}]$, respectively. In the items below, we will point out a few important observations from these results.

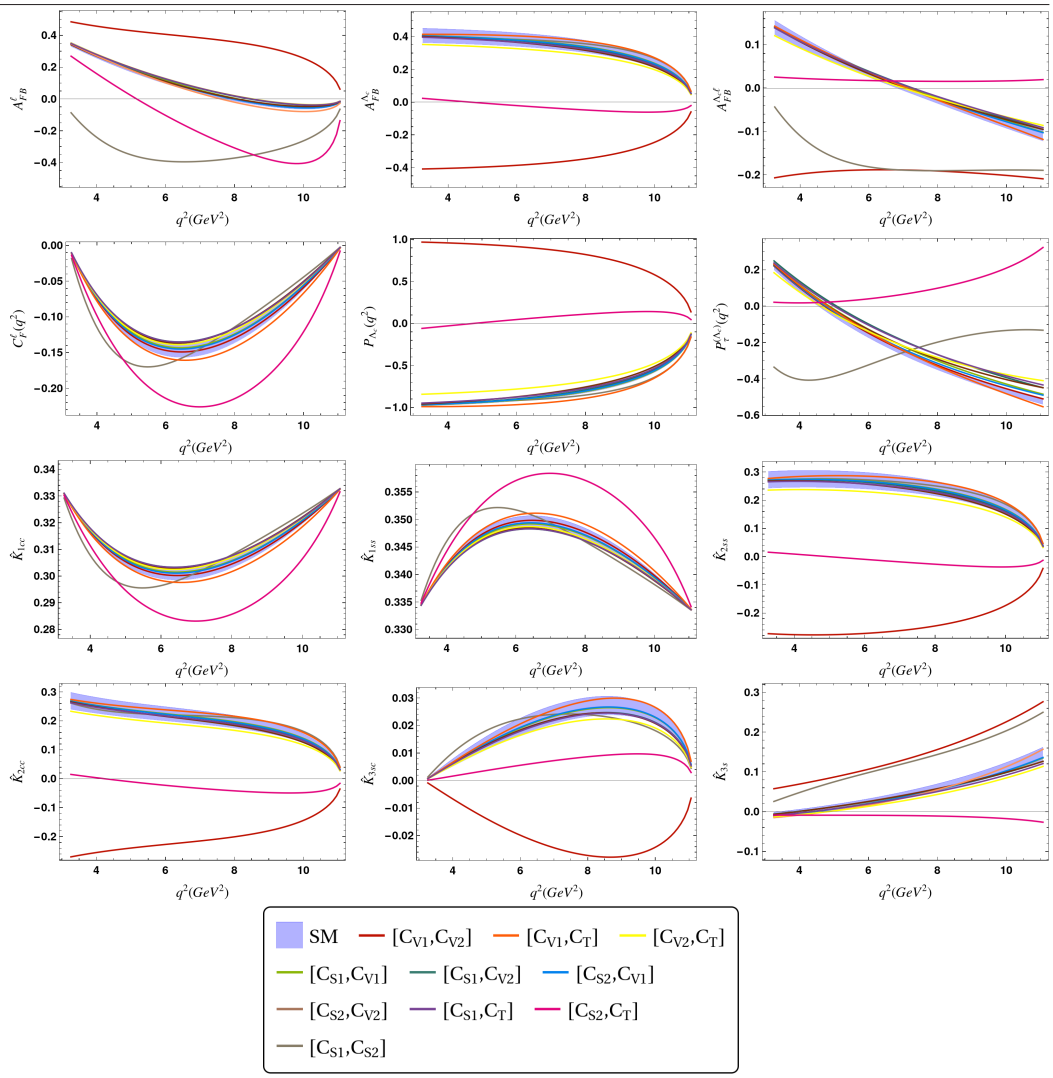

Figure 3: The q^2 dependence of the angular observables for $\Lambda_b \to \Lambda_c^+(\to \Lambda\pi^+)\tau^-\bar{\nu}_\tau$ decay. The variations have been shown for different NP two parameter scenarios.

Following the above discussions, we can argue that the information available in table 5 and in fig. 3 clearly show that the effects of the two operator scenarios are distinguishable from each other once we have measurements of all the observables mentioned above. Also, the observed pattern of the q^2 distributions of the observables are very different in the two-operator scenarios than those observed in the one-operator scenarios. Hence, in case we find discrepancies in a few or/or a couple of observables, the pattern of the discrepancies will help distinguish the effects of the one-operator scenario from that of two-operator scenarios.

4 Summary

We have found the analytical expressions for various asymmetric and angular observables from the angular analysis of $\Lambda_b \to \Lambda_c^+(\to \Lambda\pi^+)\ell^-\bar{\nu}$ decays in the SM and the NP scenarios. Wherever available, we have compared our analytical expressions with the literature. Using the available lattice inputs on the form factors, we have predicted all these observables alongside the decay rates and LFU ratio $R(\Lambda_c)$ integrated over the whole q^2 regions and small q^2 bins.

Using the available data on $B \to D^{(*)}\ell^-\bar{\nu}$ decays and $R(\Lambda_c)$, we have extracted the new Wilson coefficients and noticed that only the C_{S_2}, C_{V_2} one operator scenario can explain all these data simultaneously within 3σ. In our operator scenarios, we have predicted all the observables mentioned above and tested their NP sensitivities using our results of the fit. The observation of one operator scenario motivated us to look for two scenarios. We have done the fits to data using two different operator scenarios and found that scenario $[O_{S_2}, O_T]$ is the only two operator scenarios which could accommodate comfortably all the measured data simultaneously. In the other two operator scenarios, apart from $R(D^*)$, we are able to explain all the other data simultaneously if we take the uncertainties of our predictions at the 3σ level. We have studied the interesting correlations between the observables in different NP scenarios. In addition, we have studied the NP sensitivities of all the angular and asymmetric observables in all the two operator scenarios and found that many of them show distinguishable sensitivity to the operators $[O_{S_2}, O_T]$, $[O_{V_1}, O_{V_2}]$ and $[O_{S_1}, O_{S_2}]$. Also, the effects of one-operator scenarios are distinguishable from those of two-operator scenarios in these observables.

References

[1] S. Nandi, S. Sahoo, R. Sain, An Imperative study of the angular observables in $\Lambda_b^0 \to \Lambda_c^+(\to \Lambda\pi^+)\tau\bar{\nu}_\tau$ decay and probing the footprint of new physics (2024), 2403.12155.

[2] W. Detmold, C. Lehner, S. Meinel, $\Lambda_b \to p\ell^-\bar{\nu}_\ell$ and $\Lambda_b \to \Lambda_c\ell^-\bar{\nu}_\ell$ form factors from lattice QCD with relativistic heavy quarks, Phys. Rev. D **92**, 034503 (2015), 1503.01421. 10.1103/PhysRevD.92.034503

[3] S. Shivashankara, W. Wu, A. Datta, $\Lambda_b \to \Lambda_c\tau\bar{\nu}_\tau$ Decay in the Standard Model and with New Physics, Phys. Rev. D **91**, 115003 (2015), 1502.07230. 10.1103/PhysRevD.91.115003

[4] X.Q. Li, Y.D. Yang, X. Zhang, $\Lambda_b \to \Lambda_c\tau\bar{\nu}_\tau$ decay in scalar and vector leptoquark scenarios, JHEP **02**, 068 (2017), 1611.01635. 10.1007/JHEP02(2017)068

[5] A. Datta, S. Kamali, S. Meinel, A. Rashed, Phenomenology of $\Lambda_b \to \Lambda_c\tau\bar{\nu}_\tau$ using lattice QCD calculations, JHEP **08**, 131 (2017), 1702.02243. 10.1007/JHEP08(2017)131

[6] E. Di Salvo, F. Fontanelli, Z.J. Ajaltouni, Detailed Study of the Decay $\Lambda_b \to \Lambda_c\tau\bar{\nu}_\tau$, Int. J. Mod. Phys. A **33**, 1850169 (2018), 1804.05592. 10.1142/S0217751X18501695

[7] A. Ray, S. Sahoo, R. Mohanta, Probing new physics in semileptonic Λ_b decays, Phys. Rev. D **99**, 015015 (2019), 1812.08314. 10.1103/PhysRevD.99.015015

[8] N. Penalva, E. Hernández, J. Nieves, Further tests of lepton flavour universality from the charged lepton energy distribution in $b \to c$ semileptonic decays: The case of $\Lambda_b \to \Lambda_c\ell\bar{\nu}_\ell$, Phys. Rev. D **100**, 113007 (2019), 1908.02328. 10.1103/PhysRevD.100.113007

[9] M. Ferrillo, A. Mathad, P. Owen, N. Serra, Probing effects of new physics in $\Lambda_b^0 \to \Lambda_c^+\mu^-\bar{\nu}_\mu$ decays, JHEP **12**, 148 (2019), 1909.04608. 10.1007/JHEP12(2019)148

[10] X.L. Mu, Y. Li, Z.T. Zou, B. Zhu, Investigation of effects of new physics in $\Lambda_b \to \Lambda_c\tau\bar{\nu}_\tau$ decay, Phys. Rev. D **100**, 113004 (2019), 1909.10769. 10.1103/PhysRevD.100.113004

[11] P. Böer, A. Kokulu, J.N. Toelstede, D. van Dyk, Angular Analysis of \boldmath $\Lambda_b \to \Lambda_c(\to \Lambda\pi)\ell\bar{\nu}$, JHEP **12**, 082 (2019), 1907.12554. 10.1007/JHEP12(2019)082

[12] D. Bečirević, F. Jaffredo, Looking for the effects of New Physics in the $\Lambda_b \longrightarrow \Lambda_c(\to \Lambda\pi)\ell\nu$ decay mode (2022), 2209.13409.

[13] M. Fedele, M. Blanke, A. Crivellin, S. Iguro, T. Kitahara, U. Nierste, R. Watanabe, Impact of $\Lambda b \to \Lambda c \tau\nu$ measurement on new physics in $b \to c l\nu$ transitions, Phys. Rev. D **107**, 055005 (2023), 2211.14172. 10.1103/PhysRevD.107.055005

[14] S. Karmakar, S. Chattopadhyay, A. Dighe, Identifying physics beyond SMEFT in the angular distribution of $\Lambda_b \to \Lambda_c(\to \Lambda\pi)\tau\bar{\nu}_\tau$ decay (2023), 2305.16007.

[15] R. Aaij et al. (LHCb), Observation of the decay $\Lambda_b^0 \to \Lambda_c^+\tau^-\bar{\nu}_\tau$, Phys. Rev. Lett. **128**, 191803 (2022), 2201.03497. 10.1103/PhysRevLett.128.191803

[16] J.P. Lees et al. (BaBar), Evidence for an excess of $\bar{B} \to D^{(*)}\tau^-\bar{\nu}_\tau$ decays, Phys. Rev. Lett. **109**, 101802 (2012), 1205.5442. 10.1103/PhysRevLett.109.101802

[17] J.P. Lees et al. (BaBar), Measurement of an Excess of $\bar{B} \to D^{(*)}\tau^-\bar{\nu}_\tau$ Decays and Implications for Charged Higgs Bosons, Phys. Rev. D **88**, 072012 (2013), 1303.0571. 10.1103/PhysRevD.88.072012

[18] M. Huschle et al. (Belle), Measurement of the branching ratio of $\bar{B} \to D^{(*)}\tau^-\bar{\nu}_\tau$ relative to $\bar{B} \to D^{(*)}\ell^-\bar{\nu}_\ell$ decays with hadronic tagging at Belle, Phys. Rev. D **92**, 072014 (2015), 1507.03233. 10.1103/PhysRevD.92.072014

[19] Y. Sato et al. (Belle), Measurement of the branching ratio of $\bar{B}^0 \to D^{*+}\tau^-\bar{\nu}_\tau$ relative to $\bar{B}^0 \to D^{*+}\ell^-\bar{\nu}_\ell$ decays with a semileptonic tagging method, Phys. Rev. D **94**, 072007 (2016), 1607.07923. 10.1103/PhysRevD.94.072007

[20] S. Hirose et al. (Belle), Measurement of the τ lepton polarization and $R(D^*)$ in the decay $\bar{B} \to D^*\tau^-\bar{\nu}_\tau$, Phys. Rev. Lett. **118**, 211801 (2017), 1612.00529. 10.1103/PhysRevLett.118.211801

[21] S. Hirose et al. (Belle), Measurement of the τ lepton polarization and $R(D^*)$ in the decay $\bar{B} \to D^*\tau^-\bar{\nu}_\tau$ with one-prong hadronic τ decays at Belle, Phys. Rev. D **97**, 012004 (2018), 1709.00129. 10.1103/PhysRevD.97.012004

[22] G. Caria et al. (Belle), Measurement of $\mathcal{R}(D)$ and $\mathcal{R}(D^*)$ with a semileptonic tagging method, Phys. Rev. Lett. **124**, 161803 (2020), 1910.05864. 10.1103/PhysRevLett.124.161803

[23] R. Aaij et al. (LHCb), Measurement of the ratio of branching fractions $\mathcal{B}(\bar{B}^0 \to D^{*+}\tau^-\bar{\nu}_\tau)/\mathcal{B}(\bar{B}^0 \to D^{*+}\mu^-\bar{\nu}_\mu)$, Phys. Rev. Lett. **115**, 111803 (2015), [Erratum: Phys.Rev.Lett. 115, 159901 (2015)], 1506.08614. 10.1103/PhysRevLett.115.111803

[24] R. Aaij et al. (LHCb), Measurement of the ratio of the $B^0 \to D^{*-}\tau^+\nu_\tau$ and $B^0 \to D^{*-}\mu^+\nu_\mu$ branching fractions using three-prong τ-lepton decays, Phys. Rev. Lett. **120**, 171802 (2018), 1708.08856. 10.1103/PhysRevLett.120.171802

[25] R. Aaij et al. (LHCb), Test of Lepton Flavor Universality by the measurement of the $B^0 \to D^{*-}\tau^+\nu_\tau$ branching fraction using three-prong τ decays, Phys. Rev. D **97**, 072013 (2018), 1711.02505. 10.1103/PhysRevD.97.072013

[26] Measurement of the ratios of branching fractions $\mathcal{R}(D^*)$ and $\mathcal{R}(D^0)$ (2023), 2302.02886.

[27] Y.S. Amhis et al. (Heavy Flavor Averaging Group, HFLAV), Averages of b-hadron, c-hadron, and τ-lepton properties as of 2021, Phys. Rev. D **107**, 052008 (2023), 2206.07501. 10.1103/PhysRevD.107.052008

[28] I. Ray, S. Nandi, Test of new physics effects in $\bar{B} \to (D^{(*)}, \pi)\ell^-\bar{\nu}_\ell$ decays with heavy and light leptons (2023), 2305.11855.

[29] J. Abdallah et al. (DELPHI), Measurement of the Lambda0(b) decay form-factor, Phys. Lett. B **585**, 63 (2004), hep-ex/0403040. 10.1016/j.physletb.2004.01.086

[30] R. Aaij et al. (LHCb), Measurement of the D^* longitudinal polarization in $B^0 \to D^{*-}\tau^+\nu_\tau$ decays (2023), 2311.05224.

[31] J.A. Bailey et al. (MILC), B→D$\ell\nu$ form factors at nonzero recoil and $|V_{cb}|$ from 2+1-flavor lattice QCD, Phys. Rev. D **92**, 034506 (2015), 1503.07237. 10.1103/PhysRevD.92.034506

[32] H. Na, C.M. Bouchard, G.P. Lepage, C. Monahan, J. Shigemitsu (HPQCD), $B \to Dl\nu$ form factors at nonzero recoil and extraction of $|V_{cb}|$, Phys. Rev. D **92**, 054510 (2015), [Erratum: Phys.Rev.D 93, 119906 (2016)], 1505.03925. 10.1103/PhysRevD.93.119906

[33] A. Bazavov et al. (Fermilab Lattice, MILC, Fermilab Lattice, MILC), Semileptonic form factors for $B \to D^*\ell\nu$ at nonzero recoil from 2+1-flavor lattice QCD: Fermilab Lattice and MILC Collaborations, Eur. Phys. J. C **82**, 1141 (2022), [Erratum: Eur.Phys.J.C 83, 21 (2023)], 2105.14019. 10.1140/epjc/s10052-022-10984-9

[34] Y. Aoki, B. Colquhoun, H. Fukaya, S. Hashimoto, T. Kaneko, R. Kellermann, J. Koponen, E. Kou (JLQCD), $B \to D^*\ell\nu_\ell$ semileptonic form factors from lattice QCD with Möbius domain-wall quarks (2023), 2306.05657.